

Fig. 2. CRT display of the reflections in the test line. (a) Without stub. (b) With stub.

the bottom of the figure. The distance scale of the locating plot is non-linear in the present experiment, because the primary sweep frequency is increased linearly with time. If the primary sweep frequency is increased inversely proportional to time, the linear scale on the distance will be obtained when the v_p is constant over the test line. The ordinate indicates the reflection magnitude. As the unit of this axis is arbitrary, the reflection magnitude should be calibrated by a standard mismatch for further experiments.

Reflections are observed at the coaxial adaptor, the coaxial-to-waveguide transducer, and the stub. Furthermore, the reflection effect of the stub is clearly manifested. From the results, distance resolution at the coaxial adaptor is about 18 cm, at the transducer 31 cm, and at the stub 74 cm. The distance resolution drops quasi-linearly with distance different from the other reflectometers [1]-[3]. The reason is given as follows. In the present method, the distance resolution is mainly limited by two factors; the swept microwave bandwidth Δf and the bandpass filter's Q . The former is a fundamental limiting value on distance resolution, and universally applicable to all types of locating devices (in time domain, the rise time of the step function or the width of the spectrum of the pulse). It has been shown [1] that the shape of a reflection spectrum is approximately given by the function $|\sin x/x|$: $x = 2\pi\Delta f l/v_p$, where l is the distance from the center of the reflection spectrum. The resolution distance Δl (bandwidth of the main lobe) of the reflection is obtained from the equation $|\sin x/x| = 0.5$. The result is given as follows with rough approximation:

$$\Delta l \approx \sqrt{3}v_p/\pi\Delta f. \quad (3)$$

This equation indicates that the resolution is subjected to the swept bandwidth Δf , and the wider the swept bandwidth Δf , the better the resolution becomes. However, as the wide bandwidth sweep involves the unneigligible frequency characteristics, which elicit the error in the results and impair the distance resolution, in the test line, the allowable maximum swept bandwidth should be chosen. In the used test line, the swept bandwidth 450 MHz (Δf) is nearly allowable maximum. From (3), the 450-MHz sweep gives the resolution of about 23 cm in the coaxial line, and about 48 cm in the waveguide. However, in the present method, the latter (bandpass filter's Q) injures the fundamental resolution when the resolution distance Δl is shorter than the length determined by the bandwidth of the bandpass filter, because the reflection at distance l is always detected by the 1-kHz bandpass filter, and the filter's bandwidth determines the practical resolution. Now the resolution distance Δl is given by

$$\Delta l = \lambda_r l/Q \quad (4)$$

where λ_r is the waveguide-wavelength ratio for free space. Finally, the axial resolution drops quasi-linearly with distance in the present method. The experimental results on the axial resolution approximately agree with the results calculated from (3) and (4).

When the axial resolution is impaired by the filter's Q , the narrower bandwidth of the filter will improve the resolution. However, practical minimum bandwidth exists, because narrower bandwidth than the primary sweep frequency f_r resolves the primary sweep frequency f_r in the beat signal since the beat signal is modulated (repeated) with the primary sweep frequency f_r , and spurious spectra appear around the main reflection spectrum. This aspect complicates the interpretation of the results, therefore, f_r is the practical minimum bandwidth.

There are no limitations of measurable distance in the DSF locating reflectometer since the mechanical scanning component [2], whose movable length limits the measurable distance, is not involved in the present method. As we make the secondary sweep signal frequency lowered, the farther reflection can be detected.

The capability of measuring the small reflection is determined by the S/N value of the whole measuring system. In our experimental set, it is certified to be possible to measure the reflection coefficient of 0.0001 or less.

Though the DSF locating reflectometer does not include the function of Smith chart display [1], [2], it might be the minimum of equipment for the purpose of obtaining reflection locations and the magnitudes.

CONCLUSION

The DSF locating reflectometer makes it possible to obtain the locating plot of the reflection in the transmission line without spectrum analysis. This reflectometer has large merit in that, though the measuring system is very simple, the reflection spectrum can be directly observed on the CRT with real time, and would be very useful for the measurements of coaxial-line or waveguide systems.

ACKNOWLEDGMENT

The authors wish to thank R. Ishige and I. Yokoshima for their useful discussions.

REFERENCES

- [1] D. L. Holloway, "The comparison reflectometer," *IEEE Trans. Microwave Theory Tech.*, vol. MTT-15, pp. 250-259, Apr. 1967.
- [2] P. I. Somlo, "The locating reflectometer," *IEEE Trans. Microwave Theory Tech.*, vol. MTT-20, pp. 105-112, Feb. 1972.
- [3] Hewlett-Packard, "Microwave test set," Tech. Data, Nov. 15, 1971.
- [4] L. N. Ridenour, Ed., *Radar System Engineering*, vol. 1. Boston, Mass.: Boston Technical, 1964, p. 144.

Slotted Line Measurements for Propagation Constant in Lossy Waveguide

FRED E. GARDIOL, SENIOR MEMBER, IEEE

Abstract—The propagation coefficient in a slotted waveguide partially loaded with a lossy dielectric can be determined accurately, in terms of the measured standing-wave pattern, by means of a computer program solving a set of transcendental equations. This determination is a necessary step in a permittivity measurement technique which was recently proposed by several authors.

A novel technique to measure the permittivity of strip materials utilizing a partially loaded slotted line was recently presented in several publications [1]-[3]. Bhartia and Hamid [1] state that the *simplicity and the greater accuracy possible in the physical measurements make this method more accurate than previous methods*. Another factor in favor of this method is that it does not require delicate

Manuscript received June 24, 1974; revised September 3, 1974. This work was supported in part by the Fonds National Suisse de la Recherche Scientifique under Grant 2.8640.73.

The author is with the Ecole Polytechnique Federale de Lausanne, CH-1007 Lausanne, Switzerland.

machining of the material to be measured. However, while the authors indicate how to determine the complex permittivity of the strip material as a function of attenuation and wavelength in the partially loaded line, no details are given as to how the latter information should be extracted from the measurement data obtained from a slotted line partially loaded with lossy material. This apparent omission is considered in the present short paper which presents a computer method for the evaluation of the propagation coefficient (attenuation and phase) when the extrema of the standing-wave pattern have been measured (location and amplitude).

For a lossless dielectric in a lossless slotted line, the determination of wavelength is straightforward: it is twice the distance between minima (or maxima); for a line terminated into a short circuit, the minima are very sharp (zeros), and easy to locate accurately. Matters are no longer as simple when a lossy insert is placed within the waveguide: the distance between minima (when there are minima) is no longer a half-wavelength, except, approximately, for very low losses and measurements made very close to the short-circuited termination. Even then, significant errors could be made [4]. Outside of this limiting case, the determination of the attenuation and of the wavelength requires the simultaneous resolution of a set of transcendental equations for which there is no obvious simple solution.

The signal amplitude along the slotted line has the following dependence on the direction of propagation z (the time dependence $\exp(j\omega t)$ is suppressed in the usual manner):

$$U(z) = U_0 \cosh(\gamma z + C) \quad (1)$$

where $\gamma = \alpha + j\beta$ is the propagation exponent, U_0 is a constant voltage factor, and C is a constant depending on the nature and location of the termination (which does not have to be a complete short circuit).

It must be kept in mind at this point that the usual slotted line measurements yield only the amplitude of the signal (phase information could possibly be obtained by using an additional phase bridge; however, this would necessarily complicate the method).

The square of the magnitude of the signal $U(z)$ is obtained from (1) as follows:

$$\begin{aligned} |U(z)|^2 &= U(z)U^*(z) \\ &= |U_0|^2 \cosh(\alpha z + A + j\beta z + jB) \cosh(\alpha z + A - j\beta z - jB) \\ &= (|U_0|^2/2) \{ \cosh(2\alpha z + 2A) + \cos(2\beta z + 2B) \} \quad (2) \end{aligned}$$

where $C = A + jB$, and where the asterisk $*$ denotes the complex conjugate. A graphic representation of this dependence is presented in Fig. 1, corresponding to the case $\alpha/\beta = 0.35/\pi$ with a short circuit at $z = l$. The abscissa represents the distance, expressed in terms of wavelengths, from the short-circuit termination. The square of the amplitude of the signal varies in a sine-wave pattern (of period $\pi/\beta = \lambda/2$) between the two envelopes. The wavelength and attenuation can be obtained by considering the points at which the solid line is tangent to the envelopes; these points, unfortunately, do not coincide with the extrema of the square of the magnitude.

A graphic determination would be feasible by measuring a sufficient number of amplitude values along the slotted line, drawing the complete curve, and then the envelopes; both α and β could in turn be determined. This would, however, be a long and tedious procedure, quite unsuited for measurements on a routine basis.

A more practical approach is feasible, however: i.e., by measuring the locations z_i and wave amplitudes U_i at the extrema of the standing wave and relying on the computer for the processing of the information. The positions of the extrema are obtained by setting the derivative of (2), with respect to z , equal to zero, which yields

$$\alpha \sinh(2\alpha z + 2A) = \beta \sin(2\beta z + 2B). \quad (3)$$

The locations of a number N of extrema (maxima and minima) are determined, yielding a set of values z_i with $i = 1 \dots N$ ($N \geq 4$). A set of approximate values of the constant B is then evaluated as a function of α , β , and A using the following relation:

$$B_i(\alpha, \beta, A) = \frac{1}{2} \sin^{-1} [(\alpha/\beta) \sinh(2\alpha z_i + 2A)] - \beta z_i. \quad (4)$$

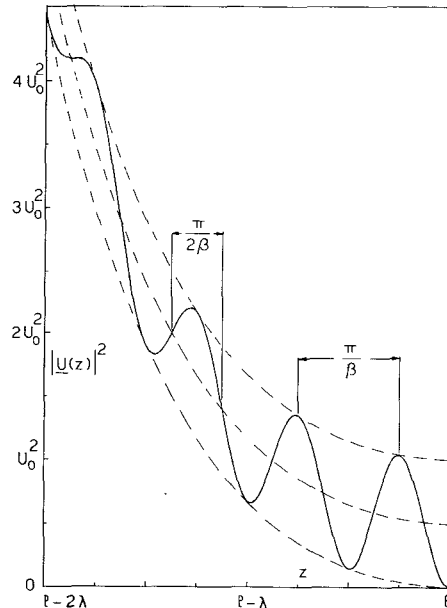


Fig. 1. Square of the voltage amplitude along a lossy line terminated with a short circuit at $z = l$ for the situation $\alpha/\beta = 0.35/\pi$.

If the true values for α , β , and A were introduced into (4), the values of all the B_i would coincide; a search technique can therefore be used to determine the values of α , β , and A which minimize (or if possible, set equal to zero) the variance of the B_i coefficients

$$f_1(\alpha, \beta, A) = \left(\sum_{i=1}^N B_i^2 / N \right) - \left(\sum_{i=1}^N B_i / N \right)^2. \quad (5)$$

The minimum of this objective function can be determined using a standard computer search technique, a number of which are currently available [5]. The search can be initiated by using a rough approximation in which three adjoining minima are assumed to correspond roughly to points of tangence of the curve with its envelope. These minima are here labeled (z_1, U_1) , (z_2, U_2) , and (z_3, U_3) , with $z_1 < z_2 < z_3$. The approximate starting values are then given by

$$\beta_0 = \frac{2\pi}{z_3 - z_1} \quad (6)$$

$$\alpha_0 = \frac{1}{z_3 - z_2} \cosh^{-1} \left(\frac{U_1^2 + U_3^2 + |U_0|^2}{2U_2^2 + |U_0|^2} \right) \quad (7)$$

$$A_0 = \coth^{-1} \frac{U_3 - U_1}{2U_2 \sinh(\alpha z_2 - \alpha z_1)} - \alpha z_2. \quad (8)$$

The approximation (6) and (7) yields first-order values which are valid in the limiting case of small attenuations.

A further step may help in checking the accuracy obtained and improving it, or alternatively, in decreasing the number of measurements needed: it consists of comparing the measured amplitudes U_i with the ones calculated from the position measurements. Different values for the voltage constant U_0 are then determined by

$$U_{0i} = \frac{U_i}{[\frac{1}{2} \cosh(2\alpha z_i + 2A) + \frac{1}{2} \cos(2\beta z_i + 2B_i)]^{1/2}}. \quad (9)$$

Here again, the N values U_{0i} obtained should coincide when the true values of the propagation exponent and the termination constant are used. Therefore, a second objective function to be minimized is given by the variance

$$f_2(\alpha, \beta, A) = \left(\sum_{i=1}^N U_{0i}^2 / N \right) - \left(\sum_{i=1}^N U_{0i} / N \right)^2. \quad (10)$$

The determination of α and β can thus be done by minimizing either function f_1 or f_2 or any suitable combination of both. For accurate measurements, the minima of both functions should coincide.

The complex permittivity of the material is then obtained by means of the program presented in [3]. By including in the computer procedure the search for α and β , one would be able to determine ϵ_r directly from the slotted line measurements (location and amplitude of the extrema). This technique, however, remains limited to those situations where the standing-wave pattern presents extrema; this is no longer the case for highly lossy materials or far from the shorted termination.

The method presented here can readily be used in other situations where the propagation coefficient is to be determined from field pattern measurements along open lines: microstrip, microslot, dielectric waveguides, G-lines, and confocal transmission lines, to name only a few.

REFERENCES

- [1] P. Bhartia and M. A. K. Hamid, "Dielectric measurements of sheet materials," *IEEE Trans. Instrum. Meas.* (Short Papers), vol. IM-22, pp. 94-95, Mar. 1973.
- [2] I. J. Bahl and H. M. Gupta, "Microwave measurement of dielectric constant of liquids and solids using partially loaded slotted waveguide," *IEEE Trans. Microwave Theory Tech.* (Short Papers), vol. MTT-22, pp. 52-54, Jan. 1974.
- [3] P. I. Somlo, "The exact numerical evaluation of the complex dielectric constant of a dielectric partially filling a waveguide," *IEEE Trans. Microwave Theory Tech. (Lett.)*, vol. MTT-22, pp. 468-469, Apr. 1974.
- [4] E. Lertes and R. Kaminski, "Zur bestimmung der komplexen Dielektrizitätskonstante von Flüssigkeiten in Koaxialleitern mittels Abtastung des stehenden Wellenfeldes innerhalb der Probe," *Arch. Tech. Mes. Ind. Messtech.*, vol. V, p. 13, Dec. 1973.
- [5] J. W. Bandler and P. A. MacDonald, "Optimization of microwave networks by razor search," *IEEE Trans. Microwave Theory Tech. (Special Issue on Computer-Oriented Microwave Practices)*, vol. MTT-17, pp. 552-562, Aug. 1969.

Measurement of the Electromagnetic-Field Components in a Rectangular Drift Tube-Loaded Cavity Using Various Perturbing Objects

F. BRUNNER, W. SCHOTT, AND H. DANIEL

Abstract—The electric-field quantities E , E_y , E_z , and the magnetic-field quantities H and H_z in a rectangular drift tube-loaded cavity resonating in the TE_{101} mode have been measured along the z direction by means of the perturbation method using a dielectric bead, a metallic disk, a metallic needle, a metallic sphere, and a ferrite disk. The relative errors for E and E_y are 3 percent; for E_z , 10 percent on the average; whereas for H and H_z , they are 10 percent at least. The ferrite disk, being superior to the metallic sphere, offers a new technique in determining magnetic-field components in cavity resonators.

I. INTRODUCTION

The fields in the second half of a rectangular cavity resonator operating in the TE_{101} mode can be used for the phase-free acceleration of charged particles, i.e., no fixed phase relation between the phases of entrance of the particles into the fields and the phases of the fields is necessary for the acceleration [1]. In Fig. 1 a cavity resonator of this type is sketched. The reference axis for the particles is a straight line at $x = a/2$, $y = b/2$ parallel to the z axis. There is a beam hole of 4-cm diameter at the front and rear plate of the resonator. The fields in the first half of the resonator are shielded by a drift tube of length $d/2$ and 4-cm diameter which is mounted at the front plate. In order to be able to calculate particle trajectories and the energy gain within the resonator, the electric and magnetic fields must be known fairly accurately in the plane $x = a/2$ around the reference axis. Using the perturbation technique, field measurements on the reference axis and on an axis at a distance of 1 cm parallel to the reference axis in the $x = a/2$ plane were made.

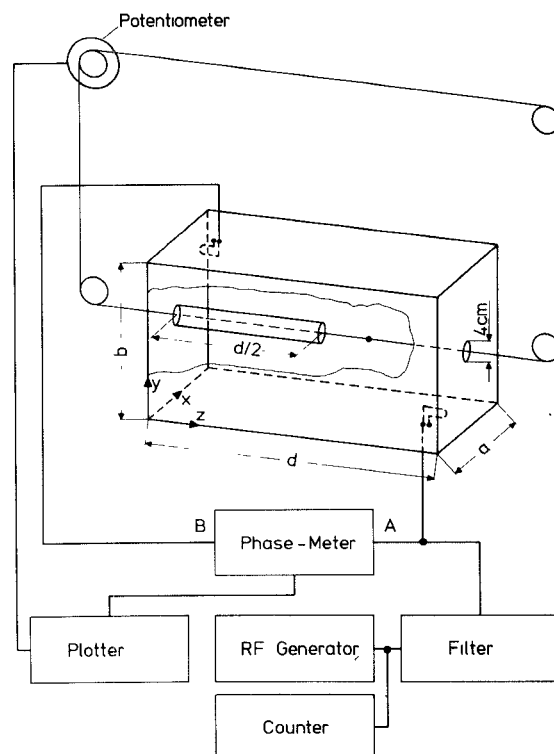


Fig. 1. Experimental setup for measuring the electromagnetic fields of a drift tube-loaded cavity resonator. The dimensions of the resonator were chosen to be $a = 25.4$, $b = 30.0$, and $d = 55.3$ cm. The drift tube has a diameter of 4 cm.

II. EXPERIMENTAL

The experimental setup is shown schematically in Fig. 1. The general perturbation method was described already by Hansen and Post [2]. Special techniques for measuring small frequency shifts in cavities were reported, e.g., by Hahn and Halama [3]. The relative frequency shift $\delta\omega/\omega$ which is caused by the perturbing object is obtained from the phase difference $\delta\phi$ between the input and output signal of the resonator by

$$\delta\omega/\omega = \delta\phi/2Q \quad (1)$$

where Q is the Q factor of the resonator. The linear relation between $\delta\phi$ and $\delta\omega/\omega$ is fulfilled within better than 1 percent if $\delta\phi$ is less than 10° . With the resonance frequency $\nu = 639.44$ MHz, the experimental Q factor $Q = 4388$, and choosing the size of the perturbing object in such a way that $\delta\phi_{\max} \approx 6^\circ$, we got for the maximum frequency shift $(\delta\omega/\omega)_{\max} \approx 1.2 \cdot 10^{-5}$. Measurements of such small frequency shifts require short measuring times to avoid a drift of the resonant frequency of the system. Therefore, a time of 1.5 min was chosen during which the perturbing object was pulled through the resonator by the pulley system. Moreover, the RF generator was quartz stabilized within 1 Hz. The position z of the perturbing object and the phase difference $\delta\phi$ were recorded by a plotter. The frequency shifts caused by ellipsoid-shaped perturbation objects are calculated and extensively reviewed in a paper by Voisin [4]. The frequency shift $(\delta\omega/\omega)_i$ caused by a special object i can be written

$$\left(\frac{\delta\omega}{\omega} \right)_i = -\pi R_i^3 \omega \left[\epsilon_0 \left(F_{||i}(\epsilon_r, \beta_i) \frac{E_{||i}^2}{PQ} + F_{\perp i}(\epsilon_r, \beta_i) \frac{E_{\perp i}^2}{PQ} \right) + \mu_0 \left(G_{||i}(\mu_r, \beta_i) \frac{H_{||i}^2}{PQ} + G_{\perp i}(\mu_r, \beta_i) \frac{H_{\perp i}^2}{PQ} \right) \right] \quad (2)$$

where $\beta_i = a_i/R_i$ is the ratio of the shorter to the longer semiaxis of the ellipsoid, and $F_{||i}$, $F_{\perp i}$, $G_{||i}$, and $G_{\perp i}$ are functions depending on the shape, the permittivity, and the permeability of the perturbing object. $E_{||i}$, $E_{\perp i}$, $H_{||i}$, and $H_{\perp i}$ are the electric- and magnetic-field